Eur. Phys. J. C (2026) 86:276
https://doi.org/10.1140/epjc/s10052-026-15432-6

THE EUROPEAN PHYSICAL JOURNAL C

Regular Article - Theoretical Physics

Islands in Kerr–Newman black holes

Ming-Hui Yu[1,a], **Xian-Hui Ge**[2,b]

[1] Department of Mathematics, Shanghai University, 99 Shangda Road, Shanghai 200444, China
[2] Department of Physics, Shanghai University, 99 Shangda Road, Shanghai 200444, China

Received: 19 November 2025 / Accepted: 10 February 2026

Abstract We investigate the information paradox in the four-dimensional Kerr–Newman black hole by employing the recently proposed island paradigm. To accurately capture the behavior of entanglement entropy in Kerr–Newman spacetime, we analyze the form of quantum fields in the near-horizon limit. We demonstrate the field can be effectively described by a reduced two-dimensional field theory. Under the framework of this reduced two-dimensional theory, the entanglement entropy of radiation satisfies the Page curve. We also examine the impact of angular momentum and charges on the Page time and the scrambling time. A step further, we concentrate on analyzing the near extremal case. Resort to the Kerr/CFT correspondence, the near-horizon geometry of near extremal Kerr–Newman black holes can be taken account for a warped AdS geometry. In this scenario, the low-energy effective degrees of freedom are dominated by the Schwarzian zero mode, resulting in a one-loop correction to the partition function. The entanglement entropy is subsequently recalculated under the thermodynamic with corrections. Through explicit calculations, we finally find that the Page time and the scrambling time exhibits quantum delays. This strongly suggests that the near extremal geometry is governed by the Schwarzian dynamics, in which quantum fluctuations result in a reduced rate of information leakage. Moreover, we provide a rigorous discussion on the validity of the island formula and compute the entanglement entropy in Kerr–Newman AdS spacetime as a supplementary example. Our findings further substantiate information conservation and extend the island paradigm to the most general class of stationary spacetime.

1 Introduction

The quantum properties of the black hole have significantly contributed to the development of a consistent theory of quantum gravity. Among these properties, one of the most intriguing is Hawking radiation, which first proposed by Stephen Hawking [1]. Since the Hawking radiation involves classical general relativity (GR) and quantum field theory, which provides a profound insight into the quantum gravity. However, Hawking radiation will eventually lead black holes to evaporate and disappear. More specifically, a black holes formed from the pure state eventually evolves into a mixed state [2]. This process violates the principle of quantum mechanics known as the unitarity, which leads to information loss [3]. The requirement of the unitarity suggests that the final state of a black hole formed by the pure state must also remain in a pure state. Consequently, this has given rise to the well-known black hole information paradox [3].

The von Neumann entropy, or the entanglement entropy, is utilized to express the quantification of the amount of information loss. Hawking's calculations in that the entanglement entropy of radiation continuously increases with time and eventually exceeds the Bekenstein–Hawking entropy bound [4] in the later stages of black hole evaporation. However, the unitary evaporation of black holes is expected to be accompanied by a particular form of the evolution of the entanglement entropy. Specifically, the entanglement entropy must asymptotically decrease to zero in end of evaporation. Based on this principle, Page demonstrates that the so-called Page curve [5] must be satisfied during the evaporation process of the entanglement entropy of Hawking radiation. Therefore, the key of resolving the black hole information paradox hinges on successfully reproducing the corresponding Page curve in the specific theoretical framework [6].

Calculating the Page curve has been a very challenging task until the proposal of the AdS/CFT duality [7]. This theory suggests that the gravitational theory in anti-de Sitter

[a] e-mail: yuminghui@shu.edu.cn
[b] e-mail: gexh@shu.edu.cn (corresponding author)

Published online: 16 March 2026

(AdS) spacetime can be equivalently described by the conformal field theory (CFT) on its boundary. This finding offers conclusive evidence that the evaporation process of black holes in AdS spacetime is unitary. Recently, this field has a significant breakthrough [8–11]. The related studies indicates that the Page curve can be calculated by the following island formula based on the quantum extremal surface (QES) prescription [12]:

$$\begin{aligned} S_R &= \min\Big[\text{ext}\big(S_{\text{gen}}\big)\Big] \\ &= \min\Big[\text{ext}\Big(\frac{\text{Area}(\partial I)}{4G_N} + S_{\text{CFT}}(R\cup I)\Big)\Big], \end{aligned} \tag{1.1}$$

where S_{gen} is denoted as the generalized entropy. It can simply be regarded as an extension of the Ryu–Takayanagi formula [13–15]. The generalized entropy is composed of the sum of the area term and the entropy associated with the quantum matter field. Here R represents the radiation region, I represents the island region with the boundary ∂I. The key to the island formula (1.1) lies in that one first extremizes the generalized entropy (ext) to obtain the position of QES, and then select the minimum value among all the candidates as the entanglement entropy of the radiation. This is also known the island paradigm [11]. Furthermore, the island formula (1.1) can be rigorously derived from the Euclidean path integral through the application of the replica trick [16–18]. Detailed calculations reveal that the emergence of the entanglement islands is associated with the replica wormholes saddle that dominates the evaporation at late times.

At present, the island paradigm has not only be applied to the initial evaporative Jackiw–Teitelboim gravity [19,20] but also extends to scenarios involving eternal black holes [21] and various specific spacetime background [22–112]. However, in these studies, nearly all have focused on the case of black holes that are *static spherically symmetric* [22–31,53–104]. There are few reports on *non-spherically symmetric* stationary black holes [61,62,79]. For the most general type in four-dimensional spacetime, known as the Kerr–Newman black hole. Its metric describes a rotating, charged mass and represents the most general solution to the Einstein's equations in GR. Therefore, it holds significant theoretical importance in the mathematical framework of GR and extends beyond. Correspondingly, resolving the information paradox in this black hole is a critical issue. This study can also offer valuable insights into other four-dimensional scenarios. Therefore, the first motivation of our study is to extend previous works to the *stationary non-spherically symmetric* Kerr–Newman spacetime. Our second motivation is to examine the behavior of the results for the near extremal case. Since for the extremal Kerr metric, the near-horizon geometry can be effectively described in a warp AdS_3. Accordingly, the calculation process and results in non-extreme cases need to corrected. Our final explicit calculation yields the corrected results and provides consistent support for unitarity.

The structure of this paper is organized as follows. In Sect. 2, we briefly review the fundamental properties of the Kerr–Newman black hole and introduce the standard technique that can transform a quantum field in the four-dimensional Kerr–Newman spacetime into an effective two-dimensional description. This approach establishes an effective two-dimensional metric near the event horizon, which facilitates the subsequent calculation of the entanglement entropy. In Sect. 3, we rigorously calculate the entanglement entropy of the radiation emitted by non-extremal Kerr–Newman black holes and derive the corresponding Page curve. Furthermore, we analyze the effects of the charge and the angular momentum on both the Page time and the scrambling time. In Sect. 4, we focus on the near extremal cases. Based on the Kerr/CFT correspondence, the near extremal Kerr–Newman geometry approximates to a warped AdS_3 at the near-horizon region. By incorporating the one-loop correction to the modified thermodynamics through the zero mode associated with Schwarzian dynamics, we arrive at a final result of Page time and scrambling time. We find these quantities will be significantly delayed due to the one-loop correction and provide the correct result in the near extremal limit. Furthermore, in Sect. 5, we provide a rigorous analysis of the regime of validity of the island formula, and present the entanglement entropy in Kerr–Newman–AdS spacetime as a supplementary example. Our results further support information conservation and demonstrate that the island paradigm remains applicable in the most general class of stationary spacetime backgrounds. Finally, the Sect. 6 summarizes the conclusions and provides further discussions.

2 Quantum fields in Kerr–Newman spacetime

In this section, we provide a concise review of the Kerr–Newman spacetime and its distinctive properties. Subsequently, we provide a detailed description of the method used to reduce a four-dimensional theory to an effective two-dimensional theory by employing the near-horizon limit. Then, the subsequent calculation of entanglement entropy can be simplified.

2.1 Kerr–Newman black black holes

In this subsection, we provide some useful relations of Kerr–Newman black holes, which are used in the following content. The metric for the rotating charged Kerr–Newman spacetime in the Boyer–Lindquist coordinate are written as follows

$$ds^2 = -\frac{\Delta - a^2\sin^2\theta}{\Sigma}dt^2 - \frac{2a\sin^2\theta(r^2+a^2-\Delta)}{\Sigma}dtd\phi$$

$$+\frac{(r^2+a^2)^2-\Delta a^2\sin^2\theta}{\Sigma}\sin^2\theta d\phi^2+\frac{\Sigma}{\Delta}dr^2+\Sigma d\theta^2, \quad (2.1)$$

where these notations are respectively defined by

$$a\equiv\frac{L}{M}, \quad (2.2a)$$
$$\Sigma\equiv r^2+a^2\cos^2\theta, \quad (2.2b)$$
$$\Delta\equiv r^2-2Mr+a^2+Q^2=(r-r_+)(r-r_-). \quad (2.2c)$$

In the above equations, M, J, Q and $r_\pm$ correspond to mass, angular momentum, charge and event(outer)/inner horizons, respectively. Moreover,

$$r_\pm=M\pm\sqrt{M^2-a^2-Q^2}. \quad (2.3)$$

For the general case, the condition $0\leq a^2+Q^2<M^2$ describes the non-extremal black hole. However, it should to notice that two horizons coincide when $M^2=a^2+Q^2$. It represents for the extremal case. The surface gravity κ is related to the Killing vector ξ^μ of the event horizon

$$\kappa(r)=\sqrt{-\frac{1}{2}\nabla^\mu\xi^\nu\nabla_\mu\xi_\nu}=\frac{r_+-r_-}{2(r^2+a^2)}. \quad (2.4)$$

Here $\xi^\mu=(\partial_t)^\mu+\Omega_H(\partial_\phi)^\mu$, where $\Omega_H=\frac{a}{r_+^2+a^2}$ is the angular velocity at the event horizon. The symbol ∇_μ is denoted as the covariant derivative operator. Then the Hawking temperature is derived by

$$T_H=\frac{\kappa(r_+)}{2\pi}=\frac{r_+-r_-}{4\pi(r_+^2+a^2)}. \quad (2.5)$$

The area of the event horizon is given by

$$\begin{aligned}\mathscr{A}&=\int\sqrt{-g}d\theta d\varphi=\int_0^{2\pi}d\varphi\int_0^{\pi}d\theta(r^2+a^2)\sin\theta \\ &=4\pi(r_+^2+a^2).\end{aligned} \quad (2.6)$$

Thus, the Bekenstein–Hawking entropy is read off as

$$S_{\rm BH}\equiv\frac{\mathscr{A}}{4G_N}=\frac{\pi(r_+^2+a^2)}{G_N}. \quad (2.7)$$

It needs to be emphasized that, in the extremal case, both the surface gravity (2.4) and the Hawking temperature (2.5) are vanishing. We will discuss the extremal case in detail in the subsequent section.

2.2 The effective two-dimensional theory

In this subsection, we demonstrate that the quantum filed in four-dimensional Kerr–Newman spacetime can be transformed to a two-dimensional theory by imposing the near-horizon limit.

For convenience, consider a complex scalar field $\phi^\star$ in Kerr–Newman spacetime. This action is written as

$$I=\int d^4x\sqrt{-g}g^{\mu\nu}(\partial_\mu+ieV_\mu)\phi^\star(\partial_\nu-ieV_\nu)\phi+I_{\rm int}. \quad (2.8)$$

where the first term is denoted as the kinetic term, the second term is the interaction terms. The gauge field V_μ is given by $\left(-\frac{Qr}{r^2+a^2},0,0,0\right)$. Then, we substitute the Kerr–Newman metric (2.1) to the action (2.8), yielding to [113]

$$\begin{aligned}I=&\int dtdrd\theta d\varphi\sin\theta\phi^\star\Bigg[\left(\frac{(r^2+a^2)}{\Delta}-a^2\sin^2\theta\right)\\ &\left(\partial_t+\frac{ieQr}{r^2+a^2}\right)^2+2ia\left(\frac{r^2+a^2}{\Delta}-1\right)\\ &\times\left(\partial_t+\frac{ieQr}{r^2+a^2}\right)\hat{L}_z-\partial_r\Delta\partial_r+\hat{L}^2-\frac{a^2}{\Delta}\hat{L}_z^2\Bigg]\phi+I_{\rm int},\end{aligned} \quad (2.9)$$

where we have used the angular momentum operator

$$\hat{L}=-\frac{1}{\sin\theta}\partial_\theta\sin\theta\partial_\theta-\frac{1}{\sin^2\theta}\partial_\varphi^2,\qquad \hat{L}_z=-i\partial_\varphi. \quad (2.10)$$

Then we expand the scalar field ϕ in terms of the spherical harmonics: $\phi=\sum_{l,m}\phi_{lm}(t,r)Y_{lm}(\theta,\varphi)$, we obtain

$$\begin{aligned}I=&\int dtdrd\theta d\varphi\sin\theta\sum_{l',m'}\phi^\star_{l'm'}Y^\star_{l'm'}\\ &\Bigg[\frac{(r^2+a^2)^2}{\Delta}\left(\partial_t+\frac{ieQr}{r^2+a^2}\right)^2-a^2\sin^2\theta\left(\partial_t+\frac{ieQr}{r^2+a^2}\right)^2\\ &+2ima\frac{r^2+a^2}{\Delta}\times\left(\partial_t+\frac{ieQr}{r^2+a^2}\right)\\ &-2ima\left(\partial_t+\frac{ieQr}{r^2+a^2}\right)-\partial_r\Delta\partial_r+l(l+1)-\frac{m^2a^2}{\Delta}\Bigg]\\ &\times\sum_{l,m}\phi_{lm}Y_{lm}+I_{\rm int}.\end{aligned} \quad (2.11)$$

In the above equation, the eigenvalue equation for $\hat{L}^2$ and $\hat{L}_z$ is used to simplify

$$\hat{L}^2Y_{lm}=l(l+1)Y_{lm},\qquad \hat{L}_zY_{lm}=mY_{lm}, \quad (2.12)$$

with l and m represents the azimuthal quantum number and the magnetic quantum number, respectively. Now we define the tortoise coordinate as a service for subsequent calculation

$$\begin{aligned}r_\star(r)\equiv&\int\frac{dr}{f(r)}=\int\frac{r^2+a^2}{\Delta}dr\\ &=r+\frac{(a^2+r_+^2)\log|r-r_+|-(a^2+r_-^2)\log|r-r_-|}{r_+-r_-}.\end{aligned} \quad (2.13)$$

Furthermore, we employ the near-horizon limit for the action (2.11). Near the event horizon $r\to r_+$, we have $f(r\simeq$

$r_+) = 0$ and only the dominant term in (2.11) is left, which yields

$$I(r_\star) = \int dt dr_\star d\theta d\varphi \sin\theta \sum_{l'm'} \phi^\star_{l'm'} Y^\star_{l'm'} \left[(r^2+a^2)\left(\partial_t + \frac{ieQr}{r^2+a^2}\right)^2 + 2ima\left(\partial_t + \frac{ieQr}{r^2+a^2}\right) - \partial_{r_\star}(r^2+a^2)\partial_{r_\star} - \frac{m^2a^2}{r^2+a^2}\right] \sum_{l'm'} \phi_{lm} Y_{lm}. \tag{2.14}$$

The interaction term $I_{\rm int}$ is discarded due to the fact that the kinetic term is dominate and the effective theory becomes to a high-energy state near the horizon. Then, we use the orthogonal condition for the spherical harmonics: $\int d\theta d\varphi \sin\theta Y^\star_{l'm'} Y_{lm} = \delta_{l'l}\delta_{m'm}$ in the expression (2.14) and rewrite it in terms of r

$$I(r) = -\sum_{l,m} \int dt dr (r^2+a^2)\phi^\star_{lm}\left[-\frac{r^2+a^2}{\Delta}\left(\partial_t + \frac{ieQr}{r^2+a^2} + \frac{ima}{r^2+a^2}\right)^2 + \partial_r \frac{\Delta}{r^2+a^2}\partial_r\right]\phi_{lm}. \tag{2.15}$$

Eventually, we can regard ϕ_{lm} as a two-dimensional complex scalar field in a two-dimensional spherical symmetric metric $g_{\mu\nu}$ with the dilaton Φ and two $U(1)$ gauge fields U, V:

$$\phi = r^2 + a^2, \tag{2.16a}$$

$$-g_{tt} = \frac{1}{g_r r} = f(r), \qquad g_{rt} = 0, \tag{2.16b}$$

$$\mathrm{U}_t = -\frac{a}{r^2+a^2}, \qquad \mathrm{U}_r = 0, \tag{2.16c}$$

$$\mathrm{V}_t = -\frac{Qr}{r^2+a^2}, \qquad \mathrm{V}_r = 0. \tag{2.16d}$$

In fact, the gauge filed V_μ is the original gauge field in the action (2.8). The other U_μ is the induced gauge field related to the isometry along the φ direction with the $U(1)$ charge m. Therefore, the gauge potential A_t is the sum of them

$$A_t = e\mathrm{V}_t + m\mathrm{U}_t = -\left(\frac{eQr + ma}{r^2+a^2}\right), \qquad A_r = 0. \tag{2.17}$$

In the end, through this set of procedures, we utilize the two-dimensional spherically symmetric effective theory at the near-horizon limit ($r \sim r_+$) to describe the behavior of quantum fields in four-dimensional non-spherical symmetric Kerr–Newman spacetime (2.1) :

$$ds^2_{\rm eff} = -f(r)d\tau^2 + f^{-1}(r)dr^2 = -\frac{(r-r_+)(r-r_-)}{r^2+a^2}d\tau^2 + \frac{r^2+a^2}{(r-r_+)(r-r_-)}dr^2. \tag{2.18}$$

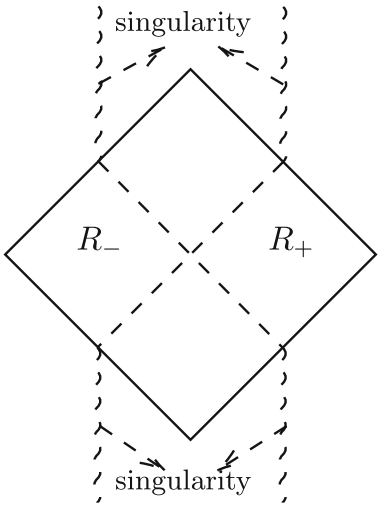

Fig. 1 The Penrose diagram for Kerr–Newman black holes. These dash lines are labeled by event horizons, which divides the whole spacetime into four wedges. $R_\pm$ represents the left and right wedge where Hawking radiation exists

The correctness of this result can be verified by calculating the Hawking temperature, which is given by

$$T_H \equiv \left.\frac{f'(r)}{4\pi}\right|_{r=r_+} = \frac{r_+ - r_-}{4\pi(r_+^2+a^2)}. \tag{2.19}$$

This temperature derived by the metric (2.18) is consistent with the temperature (2.5). Therefore, we use the effective theory (2.18) to calculate the entanglement entropy in the following content.

2.3 Conformal flat form for non-extremal case

Now, we have the effective two-dimensional metric (2.18) to describe the quantum filed in four-dimensional Kerr–Newman spacetime. In order to facilitate subsequent calculations and obtain the extension of spacetime, we need to employ the Kruskal transformation. In this section, we only focus on the non-extremal black hole. For the extremal case, we will discuss this in the Sect. 4. For the Kerr–Newman spacetime, the corresponding Penrose diagram is shown in Fig. 1.

For the non-extremal case, the tortoise coordinate is defined by (2.13). The, define the null coordinate $\{u, v\}$: $u = \tau - r_\star$, $v = \tau + r_\star$. Accordingly, the Kruskal coordinate $\{U, V\}$ that can eliminate the coordinate singularities are written as

$$\begin{aligned} &\text{Left Wedge}: \quad U \equiv +e^{-\kappa u}; \qquad V \equiv -e^{+\kappa v}. \\ &\text{Right Wedge}: \quad U \equiv -e^{-\kappa u}; \qquad V \equiv +e^{+\kappa v}. \end{aligned} \tag{2.20}$$

Under this transformation, the effective metric (2.18) becomes to a conformal flat form

$$ds^2 = -\frac{dUdV}{\Omega^2(r)}, \tag{2.21}$$

with the conformal factor $\Omega(r)$

$$\Omega(r) \equiv \frac{\kappa e^{\kappa r_\star(r)}}{\sqrt{f(r)}}. \tag{2.22}$$

In addition, the geodesic distance $L(a, b)$ between two points a and b in the conformal flat metric (2.21) is given by

$$L^2(a,b) = \frac{1}{\Omega(a)\Omega(b)}\Big(U(b) - U(a)\Big)\Big(V(a) - V(b)\Big). \tag{2.23}$$

3 Page curves for non-extremal Kerr–Newman black holes

In this section, we provide the explicit calculation of the entanglement entropy in Kerr–Newman spacetime. For simplicity, we only consider the quantum field in the non-extremal case (2.18) in this section. In addition, it is essential to emphasize some concrete calculation details. It is widely recognized that deriving the analytical expression of entanglement entropy in four-dimensional or higher dimensional spacetime poses a challenging task. We typically employ the s-wave approximation [59] to neglect the contributions from the angular direction, thereby allowing us to concentrate on the dominance of the radial direction. Therefore, the effective two-dimensional theory (2.18) derived from the near-horizon approximation well conforms to this point. Namely, the behavior of the entanglement entropy for Kerr–Neman black holes is described by this theory (2.18) equivalently in the near-horizon region. On the other hand, we assume that the radiation region is described by conformal fields with the central charge c. To disregard the back-reaction of Hawking radiation on spacetime, we further assume that black holes are semi-classical, i.e., the relationship between the mass M and the central charge satisfies: $1 \ll c \ll M \sim \frac{1}{G_N}$. Under these assumptions, the dynamics of radiation region are subject to the CFT_2. Finally, by neglecting the gray-body factor of Hawking radiation, the entanglement entropy in four-dimensional Kerr–Newman spacetime can be approximately obtained by CFT_2.

3.1 Entanglement entropy without island

We now assume that black holes formed by the pure state and calculate the entanglement entropy. The Penrose diagram is shown in Fig. 2. We first consider the construction without entanglement island. In this case, only the radiation are left in the whole spacetime. We denote the boundary point for

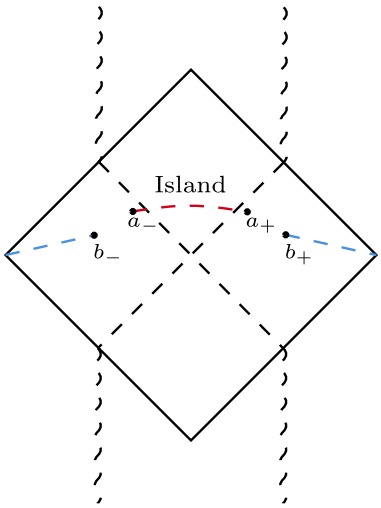

Fig. 2 The Penrose diagram for non-extremal Kerr–Newman black holes by considering the entanglement island. The blue line represents the region of radiation where the Hawking radiation is collected by the asymptotical observer. The red line represents the region of island. The points $a_\pm/b_\pm$ are denoted by endpoints of island/radiation

radiation are $b_\pm$. The coordinate for b_+ is $(\tau, r) = (t_b, r_b)$, and for b_- is $(\tau, r) = (-t_b + \frac{i\beta}{2}, r_b)$, where $\beta = \frac{1}{T_H}$ is the inverse temperature (2.5).

In the absent of island, we need to calculate the interval of radiation $(-\infty, b_-) \cup (b_+, \infty)$. Based on the complementary of entanglement entropy. The entropy in this interval equals to the complementary interval (b_-, b_+). Therefore, the entanglement entropy for a single interval in CFT_2 is determined by the logarithmic law [114]

$$\begin{aligned} S_{\text{CFT}}(R) &= \frac{c}{3}\log L(b_-, b_+) \\ &= \frac{c}{3}\log\frac{\Big[U(b_-) - U(b_+)\Big]\Big[V(b_+) - V(b_-)\Big]}{\Omega(b_-)\Omega(b_+)}. \end{aligned} \tag{3.1}$$

We substitute the related expression (2.22) and the coordinate of (b_-, b_+), yield to

$$S_{\text{CFT}}(R) = \frac{c}{6}\log\frac{4f(r_b)}{\kappa^2}\cosh^2(\kappa t_b). \tag{3.2}$$

Evidently, the expression without island as a function of time t_b. At late times, the above expression is approximated as

$$\begin{aligned} S_R^{\text{no-island}} &= S_{\text{CFT}}(R) \\ &= \frac{c}{6}\log\left[\frac{4(r_b - r_+)(r_b - r_-)(r_+^2 + a^2)^2}{(r_b^2 + a^2)(r_+ - r_-)^2}e^{2\kappa t_b}\right] \\ &\simeq \frac{2c}{3}\pi T_H t_b. \end{aligned} \tag{3.3}$$

Therefore, the entanglement entropy without entanglement island increases linearly with time t_b, which will even-

tually exceed the entropy bound [4] and cause information loss. For an eternal black hole, its entanglement entropy is limited to at most twice of the Bekenstein–Hawking entropy. But the result (3.3) demonstrates that entropy without island is infinite at late times. The paradox is sharpened here. In the next subsection, we recalculate the entanglement entropy by taking into account the island. It will result in the expected unitary Page curve for non-extremal Kerr–Newman black holes.

3.2 Entanglement entropy with island

Now, we consider that a single island is contained in Kerr–Newman spacetime. As shown in Fig. 2. We set the coordinates of the island region (a_-, a_+) are (t_a, r_a) for a_- and $(-t_a + \frac{i\beta}{2}, r_a)$ for a_+. According to the island formula (1.1), the contribution of entanglement entropy to the matter part originates from the union $I \cup R$, which is given by [114]

$$S_{\rm CFT}(R\cup I) = \frac{c}{6}\log\left[\frac{L(a_+,a_-)L(b_+,b_-)L(a_+,b_+)L(a_-,b_-)}{L(a_+,b_-)L(a_-,b_+)}\right]. \tag{3.4}$$

Then the first area term is written as $\frac{\text{Area}(\partial I)}{4G_N} = 4\pi(r_a^2+a^2)$ (2.6). Correspondingly, the generalized entropy is read off

$$\begin{aligned} S_{\rm gen} &= 2\frac{\text{Area}(\partial I)}{4G_N} + S_{\rm CFT}(R\cup I) \\ &= \frac{2\pi(r_a^2+a^2)}{G_N} \\ &\quad + \frac{c}{6}\log\left[\frac{16 f(r_a) f(r_b)}{\kappa^4}\cosh^2(\kappa t_a)\cosh^2(\kappa t_b)\right] \\ &\quad + \frac{c}{3}\log\left[\frac{\cosh[\kappa(r_\star(r_a)-r_\star(r_b))]-\cosh[\kappa(t_a-t_b)]}{\cosh[\kappa(r_\star(r_a)-r_\star(r_b))]+\cosh[\kappa(t_a+t_b)]}\right]. \end{aligned} \tag{3.5}$$

Here we substitute the expressions (2.22) and (2.23) into the above equation to simplify. The next step is to extremize the generalized entropy and find the location of island. However, prior to proceeding further, it is essential for us to study the generalized entropy in the early stage.

At early times, we assume that the time t_a and t_b are small enough: $t_a \simeq t_b \ll \kappa r_b$. So the entropy (3.5) behaves as

$$S_{\rm gen}(\text{early}) \simeq \frac{2\pi(r_a^2+a^2)}{G_N} + \frac{c}{6}\log \times\left[\frac{16 f(r_a) f(r_b)}{\kappa^4}\cosh^2(\kappa t_a)\cosh^2(\kappa t_b)\right]. \tag{3.6}$$

By extremizing the above expression with respect to the time t_a and the position r_a, we consequently obtain

$$\frac{\partial}{\partial t_a} S_{\rm gen}(\text{early}) = \frac{c\kappa}{3}\tanh(\kappa t_a) = 0, \tag{3.7a}$$

$$\frac{\partial}{\partial r_a} S_{\rm gen}(\text{early}) = \frac{4\pi r_a}{G_N} + \frac{c}{6}\frac{a^2(2r_a - r_+ - r_-) + r_a(r_a(r_+ + r_-) - 2r_+ r_-)}{(r_a^2+a^2)(r_a - r_+)(r_a - r_-)} = 0. \tag{3.7b}$$

At the leading order $\mathcal{O}(G_N^{-1})$, we find the coordinates of QES at early times is

$$t_a = 0, \qquad r_a \simeq \frac{cG_N}{24G_N}\frac{r_+ + r_-}{r_+ r_-} = \frac{cM}{12\pi a^2}\ell_p^2, \tag{3.8}$$

where $\ell_p = \sqrt{G_N}$ is denoted as the four-dimensional Planck length. Our calculation should exclude the physics at the Planck scale. Therefore, indeed, the island is nonexistent at early times. The entanglement entropy is only determined by the radiation (3.3). Namely, the construction without island always lead to information paradox.

Next, we turn our attention to the later stage of evaporation. The island that emerges at late times constitute the necessary and sufficient condition for the existence of Page curves. At late times, the time scales t_a and t_b are big enough: $t_a, b \gg \kappa r_b$. Due to the fact that the distance between the left wedge R_- and the right wedge R_+ becomes significantly large at this moment. The following approximation can be obtained

$$\begin{aligned} L(a_+,a_-) &\simeq L(b_+,b_-) \simeq L(a_+,b_-) \\ &\simeq L(a_-,b_+) \gg L(a_\pm,b_\pm). \end{aligned} \tag{3.9}$$

Under this approximation, the generalized entropy (3.5) is reduced to

$$S_{\rm gen}(\text{late}) = \frac{2\pi(r_a^2+a^2)}{G_N} + \frac{c}{6}\log\left[\frac{4 f(r_a) f(r_b)}{\kappa^4}\left(\cosh\left(\kappa(r_\star(r_a)-r_\star(r_b))\right)-\cosh\left(\kappa(t_a-t_b)\right)\right)^2\right]. \tag{3.10}$$

Similarly, extremizing this expression with respect to time t_a first

$$\frac{\partial}{\partial t_a} S_{\rm gen}(\text{late}) = -\frac{c}{3}\frac{\kappa\sinh[\kappa(t_a-t_b)]}{\cosh[\kappa\left(r_\star(r_a)-r_\star(r_b)\right)]-\cosh[\kappa(t_a-t_b)]} = 0. \tag{3.11}$$

By solving this equation, we find that $t_a = t_b$. Invoking the relation $t_a = t_b = t$ into the expression (3.10) and extremize

it with respect to r_a

$$\frac{\partial}{\partial r_a} S_{\rm gen}(\text{late}) = \frac{4\pi r_a}{G_N} + \frac{c}{6}\frac{a^2(2r_a - r_+ - r_-) + r_a(r_a(r_+ + r_-) - 2r_+r_-)}{(r_a^2 + a^2)(r_a - r_+)(r_a - r_-)} - \frac{c\kappa(r_a^2 + a^2)}{3(r_a - r_+)(r_a - r_-)}\left(1 + \frac{2}{e^{\kappa x} - 1}\right) = 0, \tag{3.12}$$

where $x \equiv r_\star(r_b) - r_\star(r_a)$. Subsequently, we take the near-horizon limit: $a \simeq r_+$, yield to

$$f(r) \simeq f'(r_+)(r - r_+) + \mathcal{O}[(r - r_+)^2] = 2\kappa(r - r_+) + \mathcal{O}[(r_- r_+)^2]. \tag{3.13a}$$

$$r_\star(r) = \int \frac{dr}{f(r)} \simeq \frac{1}{2\kappa}\log\frac{|r - r_+|}{r_+}. \tag{3.13b}$$

Substituting these relations into the Eq. (3.12), we obtain the following equation

$$\frac{\partial}{\partial r_a} S_{\rm gen}(\text{late}) \simeq 24\pi\kappa r_a(r_a - r_+) - 2cG_N\kappa e^{-\kappa r_\star(r_b)} + \frac{a^2 - r_+(r_+ - 2r_-)}{(a^2 + r_+^2)^2}(r_a - r_+)cG_N = 0. \tag{3.14}$$

At last, the location of island is obtained by solving this equation

$$r_a \simeq r_+ + \frac{c^2 G_N^2}{144\pi^2 r_+^3}\frac{r_b - r_-}{r_b - r_-} e^{\frac{-r_b(r_+ - r_-)}{r_+^2 + a^2}} + \mathcal{O}[(cG_N)^3] \simeq r_+ + \frac{c^2}{144\pi^2 r_+^3}\ell_p^2. \tag{3.15}$$

We find that the distance at which the boundary of island extends beyond the event horizon is limited to the Planck scale, which conforms the near-horizon approximation (3.13a) (3.13b). Correspondingly, the entanglement entropy of radiation after considering the contribution of island is

$$S_R^{\rm island} \simeq \frac{2\pi(r_+^2 + a^2)}{G_N} + \frac{c}{6}\log\left[\frac{4c^2 G_N^2(r_b - r_+)(r_b - r_-)(a^2 + r_+^2)}{9\pi^2 r_+^3(r_+ - r_-)^3(a^2 + r_b^2)}\right] = 2S_{\rm BH} + \mathcal{O}(cG_N). \tag{3.16}$$

Namely, the entanglement entropy is dominated by the area term $\frac{\text{Area}(\partial I)}{2G_N}$ at late times, which is consistent with the Bekenstein–Hawking entropy bound. The remaining subleading term arise from the contribution of the matter field and can be neglected compared to the leading term. Therefore, entropy with entanglement island eventually asymptotes to twice the Bekenstein–Hawking entropy of an eternal Kerr–Newman black hole. Combing the prior findings without entanglement island (3.3), we summarize the behavior of entanglement entropy: In the early stage, the entropy increases approximately in a linear manner. In the later stage, the growth of entropy cease. Eventually, the entropy of Hawking radiation is bounded by the Bekenstein–Hawking entropy, which is consistent with the unitarity. Therefore, the information paradox of non-extremal Kerr–Newman black holes can be solve by plotting the corresponding Page curve as shown in Fig. 3.

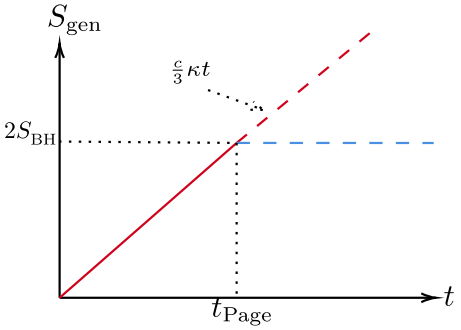

Fig. 3 The time evolution of entanglement entropy of non-extremal eternal Kerr–Newman black holes. The red line represents the entropy without island. While the blue line represents the entropy with a single island. The Page curve is represented by the solid line

3.3 Page time and scrambling time

Finally, we provide the Page time and the scrambling time as by-products of Page curves. The Page time is defined by the moment when the entanglement entropy reduces maximum. For an evaporating black hole, its entanglement entropy will decrease after the Page time. While for an eternal black hole, the entanglement entropy keeps a saturation value after this time. We can determine the Page time by comparing the entropy without island (3.3) and the entropy with island (3.16):

$$t_{\rm Page}(a, Q) = \frac{6}{c\kappa}S_{\rm BH} = \frac{3\beta}{\pi c}S_{\rm BH} = \frac{12\pi}{cG_N}\frac{(r_+^2 + a^2)^2}{(r_+ - r_-)} = \frac{6\pi}{cG_N}\frac{\left[a^2 + \left(M + \sqrt{M^2 - a^2 - Q^2}\right)^2\right]^2}{\sqrt{M^2 - a^2 - Q^2}}. \tag{3.17}$$

In particular, for the special case when $a = 0$ (RN black holes) and $Q = 0$ (Kerr black holes), our results are consistent with the previous work [60,61]. This further corroborates the validity of our calculations. Then we plot the Page time as a function of the angular momentum a and the charge Q in Fig. 4.

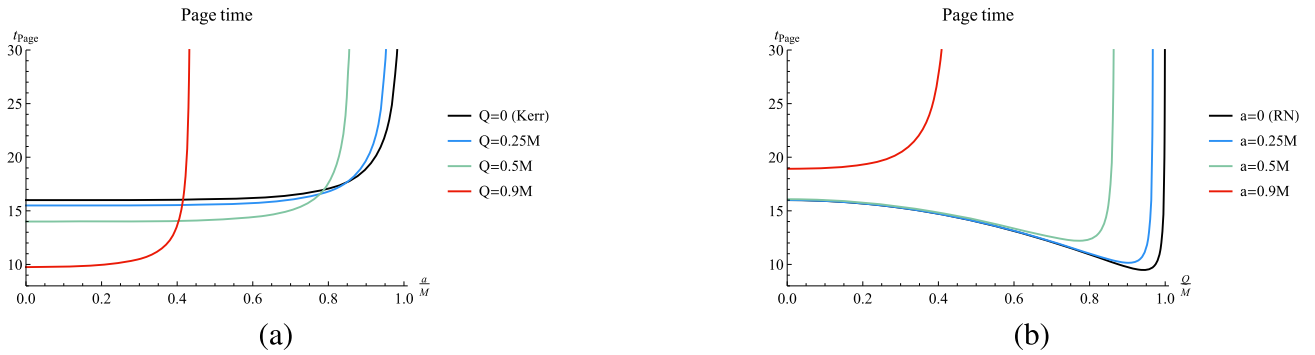

Fig. 4 The Page time as a function for the angular momentum a and the charge Q (in the unit of $\frac{6\pi}{cG_N}$). On the left, the charge Q is fixed; On the right, the angular momentum a is fixed. Note that in the extremal case, the Page time is divergent

We find that the Page time increases as the angular momentum a increases, but decreases as the charge Q increases. However, when the charge or the angular momentum reaches a sufficiently large value, the Kerr–Newman black holes becomes extremal. At this stage, the Page time exhibits divergent. A concrete discussion of the extremal case is provided in the subsequent section.

Further, we discuss the scrambling time. Based on the Hayden–Preskill experiment, for an observer located outside the event horizon, (s)he must wait for the so-called "scrambling time" to recover the quantum information that has fallen into the black hole via the emitted Hawking radiation [115]. On the other hand, according to the entanglement wedge reconstruction proposal [10], the scrambling time corresponds to the time when the information reaches the boundary of entanglement islands. Since the entanglement wedge of black hole interior constitutes a portion of the entanglement wedge associated with external radiation. Thus, at time t_1, suppose an observer at the cut-off surface $r = r_b$ transmits a light signal toward the black hole. Assuming that the information carried by this signal can be instantaneously decoded upon entering black holes. Then the time at which the information reaches the island $r = r_a$ is denotes as t_2. In the null direction, the geodesic distance between these two events is written as

$$v(t_1, r_b) - v(t_2, r_a) = [t_1 + r_\star(r_b)] - [t_2 + r_\star(r_a)]. \quad (3.18)$$

There, the scrambling time is defined by the shortest time interval $\Delta t = t_2 - t_1$

$$\begin{aligned} t_{\rm scr} &\equiv \min[\Delta t] \\ &= \min\Big[\big(r_\star(r_b) - r_\star(r_a)\big) - \big(v(t_1, r_b) - v(t_2, r_a)\big)\Big] \\ &= r_\star(r_b) - r_\star(r_a), \end{aligned} \quad (3.19)$$

We take the location of island (3.15) into the expression and obtain

$$\begin{aligned} t_{\rm scr}(a, Q) &= \frac{a^2 + r_+^2}{2(r_+ - r_-)} \log\left[\frac{144\pi^2 (r_b - r_+)(r_+^2 + a^2)^2}{c^2 G_N^2 (r_b - r_-)}\right] \\ &\simeq \frac{1}{2\kappa} \log S_{\rm BH} + \frac{1}{2\kappa} \log\left[\frac{12\pi (r_b - r_+)}{c(r_b - r_-)}\right] \\ &\simeq \frac{\left[\left(M + \sqrt{M^2 - a^2 - Q^2}\right)^2 + a^2\right]}{2\sqrt{M^2 - a^2 - Q^2}} \\ &\quad \log\left[\frac{\pi\left[a^2 + (M + \sqrt{M^2 - a^2 - Q^2})^2\right]}{G_N}\right]. \end{aligned} \quad (3.20)$$

At the leading order, the result $\frac{1}{2\kappa} \log S_{\rm BH}$ is agree with the Hayden–Preskill experiment [116,117]. The scrambling time is logarithmically less the the Page time (3.17). Therefore, it can be neglected throughout the whole evaporating lifetime. Similarly, for the special cases $a = 0$ and $Q = 0$, the above results is also consistent with pervious studies [60,61]. We also plot the function of the scrambling time as the function of Q and a in Fig. 5. The behavior of scrambling time exhibits similarities to that of the Page time. It increases as the angular momentum rises and decreases as charges increases. In the same way, the scrambling time also becomes divergent in the extremal case. We leave this point for discussion in the next section.

4 Near horizon of near extremal black holes

Up to now, we have reproduce the Page curve for the non-extremal Kerr–Newman black hole and obtain the Page time (3.17) and the scrambling time (3.20). However, it is evident from Figs. 4 and 5 that when the charges or angular momentum is large to render the black hole becomes near extremal, the corresponding physical quantities are divergent and ill-defined. Due to the fact that the distinct spacetime structures of extremal black holes and non-extremal black holes, there exist fundamental differences between the two types [118]. Furthermore, For a near extremal black at low or vanishing temperature, a serious problem exists: The internal energy E increases quadratically from the extremal

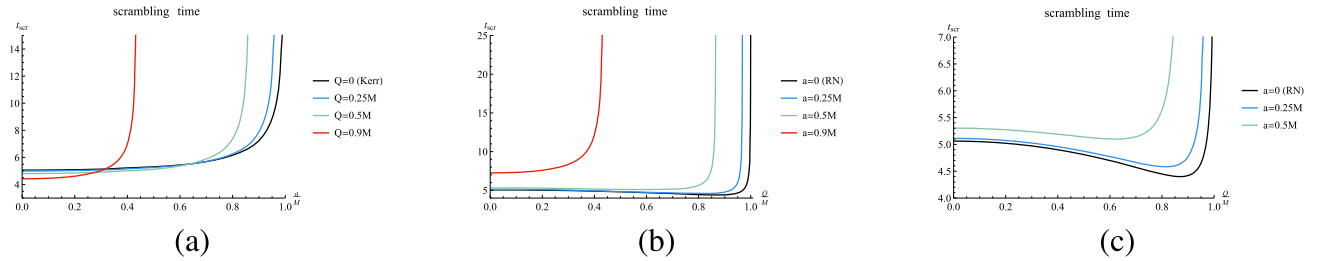

(a) (b) (c)

Fig. 5 The scrambling time as a function for the angular momentum a and the charge Q. Here we set $G_N = 1$. **a** The charge is fixed. **b** The angular momentum is fixed. **c** Is the zoomed plot of **b**

value, namely, $E \sim \frac{T_H^2}{M_{\text{gap}}}$. This suggests the presence of a mass gap of order M_{gap} in the microscopic spectrum. Consequently, it is expected that a near extremal black hole at temperatures below this gap scale cannot emit the Hawking quantum in the canonical ensemble, where the charges are fixed [119]. Therefore, in this section, we focus on the near extremal case and carefully investigate the behavior of entanglement entropy in this scenario. Finally, we provide the precise expressions of entropy, Page time and scrambling time in the near extremal case.

Firstly, we consider the case of near extremal black holes. Then the corresponding results for extremal cases can be derived by the limiting analysis. Note that the island is actually located in close proximity to the horizon (3.15). Therefore, we are interested in the near-horizon Kerr–Newman geometry. In this situation, these exists a significant correspondence, which is called the Kerr/CFT correspondence [120]. This conjecture suggests that under specific boundary conditions, quantum gravity theory in the near-horizon near extremal Kerr geometry is dual to a two-dimensional chiral CFT. This originated from the investigation of asymptotic symmetry groups in the near-horizon geometry of near extremal Kerr black holes. By imposing a definite boundary condition on the asymptotic behavior of the metric, the $U(1)_L$ symmetry of the $SL(2, R)_R \times U(1)_L$ isometry group in the geometry is enhanced to the Virasoro algebra. For further support regarding this field, one can refer to [121,122]. In this context, the near-horizon near extremal Kerr black hole closely resemble that of a non-extremal warped AdS_3. Correspondingly, due to the presence of the warp AdS_3 structure in the near-horizon region of near extremal Kerr–Newmann black holes, the information encoded in its dual CFT can be easily accessed. One can still acquire the entanglement entropy in CFT_2 precisely. In addition, the logarithmic law (3.1) is not applicable when the observer at the near-horizon region. Instead, the entropy follows an area law [114]

$$S_{\text{CFT}}(R \cup I) = -\gamma c \frac{\text{Area}(r)}{L^2(a, b)}, \tag{4.1}$$

where γ is a constant. Back to the gravitational region, we start from the near extremal Kerr–Newman black hole. In order to derive the near horizon geometry for this case, we first consider the following co-rotating coordinate with the angular velocity Ω_H at the horizon

$$\phi \to \tilde{\phi} + \frac{a}{r_0^2 + a^2}\tilde{t}, \tag{4.2}$$

where $r_0 = r_\pm = M = \sqrt{a^2 + Q^2}$ represents the radius of event horizon for the extremal Kerr–Newman black holes. After here, we use the subscript 0 to represent various parameters in extremal cases. Then we take the near-horizon and near extremal limit with the $\epsilon \to 0$ as follows

$$r \to r_0 + \epsilon\tilde{r}, \quad t \to \frac{r_0^2 + a^2}{\epsilon}\tilde{t}, \quad M_0 \to r_0 + \epsilon^2 \frac{B}{2r_0}. \tag{4.3}$$

Here the parameter $B = \frac{r_+ - r_-}{2\epsilon}$ is fixed. Finally, the near-horizon geometry can obtained by this scaling limit [122, 123]

$$\begin{aligned} d\tilde{s}^2 = \Gamma(\theta)\Big[&-(\tilde{r}^2 - B^2)d\tilde{t}^2 + \frac{d\tilde{r}^2}{(\tilde{r}^2 - B^2)} + d\tilde{\theta}^2\Big] \\ &+\Lambda(\tilde{\theta})(d\tilde{\phi} + b\tilde{r}d\tilde{t}^2), \end{aligned} \tag{4.4}$$

with

$$\begin{aligned} &\Gamma(\theta) = r_0^2 + a^2\cos^2\theta, \quad \Lambda(\theta) = \frac{(r_0^2 + a^2)\sin^2\theta}{r_0^2 + a^2\cos^2\theta}, \\ &b = \frac{2ar_0^2}{r_0^2 + a^2}. \end{aligned} \tag{4.5}$$

Without loss of generality, we set $\tilde{\theta} = 0$ to simplify. Then $\Gamma(0) = r_h^2 + a^2$, $\Lambda(0) = 0$. The warped AdS_3 metric (4.4) becomes

$$\begin{aligned} d\tilde{s}^2\Big|_{\theta=0} &= \Gamma(0)\Big[-(\tilde{r}^2 - B^2)d\tilde{t}^2 + \frac{d\tilde{r}^2}{\tilde{r}^2 - B^2}\Big] \\ &= -(r_0^2 + a^2)(\tilde{r}^2 - B^2)d\tilde{t}^2 + \frac{(r_0^2 + a^2)d\tilde{r}^2}{\tilde{r}^2 - B^2}. \end{aligned} \tag{4.6}$$

The above spacetime (4.6) contains a warped AdS_3 structure, which allows a dual CFT to describe the near extremal Kerr Newman black at near-horizon region. The structure of spacetime is illustrated in Fig. 6.

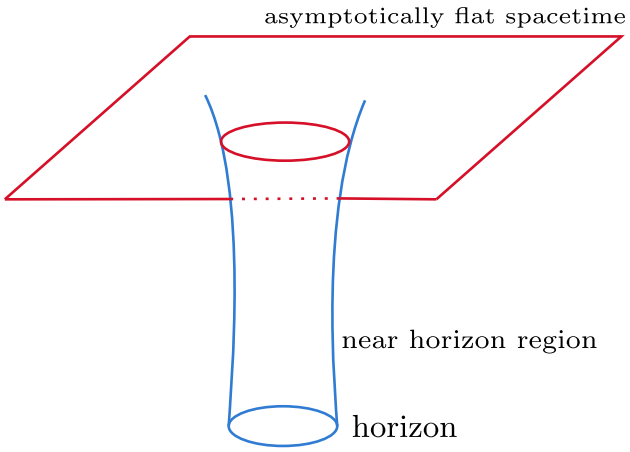

Fig. 6 The sketch of the spatial slice of the near extremal Kerr–Newman black hole. At low enough temperature, the near-horizon region is well approximated by the metric (4.4). While far away the horizon, this approximation is invalid and the metric becomes to the asymptotically flat Kerr–Newman geometry

On the other hand, for near extremal black holes, corrections to their thermodynamics at low temperature constitute another significant study [124]. At the low-temperature limit, the entropy correction of near extremal black holes primarily arises from two sources: At the classical level, this manifests as a linear temperature correction term. An additional quantum correction arises from the zero mode contribution associated with the one-loop determinant. The zero mode here is associated with large diffeomorphisms that preserve the asymptotic structure near AdS_2. Up to now, two distinct zero modes have been identified. One linked to the Schwarzian dynamics characterizing the asymptotic region of AdS_2, and the other corresponding to fluctuations in the angular velocity of black holes [125]. This relationship can be understood through the dimensional reduction on a deformed two-sphere. The first mode arises from the gravitational fluctuation in AdS_2, while the second constitutes the zero mode of the $U(1)$ Maxwell field that originate from the four-dimensional gauge field after the dimensional reduction. These findings have significantly influenced the analysis of semi-classical corrections to the thermodynamics of Kerr–Newman black holes. After considering of these two aspects, the near extremal entropy is obtained in the canonical ensemble at fixed angular momentum as follows [126]

$$\tilde{S}_{\rm BH}(\tilde{T}_H) = S_0 + a_1 \log S_0 + a_2 \log \frac{\tilde{T}_H}{T_q}, \tag{4.7}$$

where $S_0 = \frac{\mathscr{A}_0}{4G_N}$ is the extremal entropy, the coefficient a_1 and a_2 is constants of order $\mathscr{O}(1)$, $\tilde{T}_H = \frac{B}{2\pi}$ is the effective temperature at low temperature limit, and T_q is denoted a emergent scale in the IR comes from the Schwarzian dynamics. At this scale, the excitation energy of the black hole above extremality is comparable to the average energy of Hawking radiation [127]

$$T_q = \frac{\pi}{G_N M_0 S_0}. \tag{4.8}$$

It is also noteworthy that as the parameter B approaches 0, all physical quantities converge to those corresponding to the extremal case. Thus the parameter B serves as a measure of deviation from the extremal case. Thus we will subsequently take the limit of $B \to 0$ to derive the corresponding results in the extremal case.

Now we reevaluate the entanglement entropy in spacetime (4.6) to capture a more comprehensive understanding for near extremal black holes. The Kruskal transformation (2.20) is still allowed.[1] After the conformal map, the above metric (4.6) is converted as follows

$$d\tilde{s}^2 = -\tilde{\Omega}^{-2}(r) dU dV, \tag{4.9}$$

with the new conformal factor and the new tortoise coordinate

$$\tilde{\Omega}^2(r) = \frac{B^2 e^{2B\tilde{r}_\star(\tilde{r})}}{(\tilde{r}^2 - B^2)(r_0^2 + a^2)}, \quad \tilde{r}_\star(\tilde{r}) = \frac{1}{2B} \log \frac{\tilde{r} - B}{\tilde{r} + B}. \tag{4.10}$$

now we reevaluate the entanglement entropy in spacetime (4.9) to capture a more comprehensive understanding for extremal black holes. We also assume that the near extremal black hole is in a pure state at the initial time $t_0 = 0$. For the no-island configuration, the entanglement entropy dominated only by the radiation R, which is still bounded by $b_\pm$. We still need to use (3.1) to calculate the entropy due to the fact that the QES at this construction ($r_a = 0$) is far from the near-horizon region. Then, similar to (3.3), the entropy is expressed as

$$\begin{aligned} \tilde{S}_R^{\text{no-island}} &= \tilde{S}_{\rm CFT}(R) = \frac{c}{3} \log[L(b_+, b_-)] \\ &\simeq \frac{2c}{3} \tilde{T}_H \tilde{t}_b. \end{aligned} \tag{4.11}$$

So we still maintain the entropy without island increases linearly with time even in the near extremal case. Moreover, we find that in the extremal limit ($B \to 0$), this entropy becomes to zero.

We now consider the island configuration. We anticipate that the entanglement entropy of extremal Kerr–Newman black holes can retain bounded at a finite value by the island formula. After the Page time, an island region I is introduced, and its boundary is also denoted as a_+. Fortunately, based on the symmetry of the spacetime, we can investigate the

[1] For the near extremal case, note that the surface gravity $\kappa = B = \frac{r_+ - r_-}{2\epsilon}$ in the Kruskal coordinate (2.20) can not directly derived from the original expression (2.4).

complementary region (a_+, b_+), which contains no singularity [63,64]. Accordingly, the geodesic distance $L(a_+, b_+)$ is well defined and yields the correct entanglement entropy.

Here we now provide the explicit calculation. Accordingly, the generalized entropy approximates to

$$\tilde{S}_{\rm gen} = 2\frac{\text{Area}(\partial I)}{4G_N} - 2\gamma c\frac{\text{Area}(\tilde{r}_b)}{L^2(a_+,b_+)} = \frac{2\pi(\tilde{r}_a^2+a^2)}{G_N} + 2a_1\log(\tilde{r}_a^2+a^2) + 2a_2\log\frac{\tilde{T}_H}{T_q} - \frac{4\gamma c\pi\tilde{r}_b^2}{(r_0^2+a^2)\sqrt{(\tilde{r}_a^2-B^2)(\tilde{r}_b^2-B^2)}\Big[\cosh[\kappa(\tilde{r}_\star(\tilde{r}_a)-\tilde{r}_\star(\tilde{r}_b))]-\cosh[\kappa(\tilde{t}_a-\tilde{t}_b)]\Big]}. \tag{4.12}$$

We first extremize this expression with respect to time $\tilde{t}_a$, which yields

$$\frac{\partial}{\partial\tilde{t}_a}\tilde{S}_{\rm gen} \propto \sinh\left(\frac{\tilde{t}_a-\tilde{t}_b}{r_h}\right) = 0. \tag{4.13}$$

This suggest that $\tilde{t}_a = \tilde{t}_b$. Then substituting the relation into the expression (4.12) and taking the partial derivative with respect to $\tilde{r}_a$ at the near-horizon limit: $\tilde{r}_a \simeq r_h$, we obtain

$$\frac{\partial}{\partial\tilde{r}_a}\tilde{S}_{\rm gen} = \frac{4\pi\tilde{r}_a}{G_N} + \frac{4a_1\tilde{r}_a}{a^2+\tilde{r}_a^2} - \frac{2c\pi\tilde{r}_a(B-\tilde{r}_b)(B+\tilde{r}_b)\tilde{r}_b^2\gamma\,\text{csch}\left[\frac{\kappa}{2}\left(\frac{1}{\tilde{r}_b}-\frac{1}{\tilde{r}_a}\right)\right]^2}{(a^2+r_0^2)\tilde{r}_a^3\tilde{r}_b^3} = 0. \tag{4.14}$$

By solving this equation in the near-horizon limit, we obtain the location of the island is

$$\tilde{r}_a \simeq r_0 + \frac{G_N(c\pi(B-\tilde{r}_b)\gamma - 2r_0^3a_1)}{2r_0^2(a^2+r_0^2)\pi}. \tag{4.15}$$

Finally, the entanglement entropy with island for extremal case is given by

$$\tilde{S}_R^{\rm island} = \frac{2\pi(\tilde{r}_0^2+a^2)}{G_N} + 2a_1\log(\tilde{r}_0^2+a^2) + \mathcal{O}(G_N) \simeq 2\tilde{S}_{\rm BH}. \tag{4.16}$$

The entanglement entropy in the near extremal case is approximates to the Bekenstein–Hawking entropy at the leading order at late times. Then, we can determine the Page time for near extremal black hole by (4.11) and (4.16)

$$\tilde{t}_{\rm Page} = \frac{3\tilde{S}_{\rm BH}}{c\pi\tilde{T}_H} = \frac{3}{c\pi\tilde{T}_H}\left(S_0 + a_1\log S_0 + \mathcal{O}\left(\log\frac{T_q}{\tilde{T}_H}\right)\right). \simeq t_0 + t'_{\rm Page} > t_{\rm Page}. \tag{4.17}$$

Here t_0 is the Page time without considering logarithmic correction (3.17) and $t'_{\rm Page} \sim \frac{\log S_0}{\tilde{T}_H}$ originates from the logarithmic correction to the extremal entropy (4.7). In addition, the temperature correction term $\log\frac{T_q}{\tilde{T}_H}$ is neglected under the low temperature limit $\tilde{T}_H \sim T_q$. Compared with the previous results (3.17), it is observed that, in the case of near extremal black holes, the Page time is significantly delayed. This suggests that Schwarzian dynamics predominates in the near-horizon geometry of near extremal black holes and gives rise to quantum corrections to this result. Meanwhile, the scrambling time in near extremal cases can likewise be derived by the similar calculation

$$\tilde{t}_{\rm scr} = \tilde{r}_\star(\tilde{r}_b) - \tilde{r}_\star(\tilde{r}_a) = \frac{1}{2B}\log\frac{(\tilde{r}_b-B)(\tilde{r}_a+B)}{(\tilde{r}_b+B)(\tilde{r}_a-B)} \simeq \frac{1}{\tilde{r}_a} - \frac{1}{\tilde{r}_b} \simeq \frac{\tilde{r}_b-r_0}{r_0\tilde{r}_b} \sim \mathcal{O}(G_N) > t_{\rm scr} \sim \mathcal{O}(\log G_N). \tag{4.18}$$

Similar to the Page time at near extremal case (4.17). The scrambling time at this case is also be delayed compare to the previous result (3.20). Accordingly, we perform a more rigorous reanalysis of the behavior of Page time and scrambling time by employing near-horizon analysis of near extremal Kerr–Newman black holes, and provide explanations for the dependencies illustrated in Figs. 4 and 5. In particular, the entropy is still a finite value (4.16). Therefore, the island can still yield a finite entropy and ensure the unitary in extremal cases. This also implies the significance and necessity of the island paradigm.

5 Kerr Newman-AdS black hole coupled thermal bath

Up to now, we have employed the island formula (1.1) to reproduce the Page curve of the asymptotically flat four-dimensional Kerr–Newman black hole Fig. 3. In particular, for the near extremal case (4.6), we further investigate this scenario by considering the Kerr/CFT correspondence [120]. Finally, the explicit expressions for the corrected Page time (4.17) and the corrected scrambling time (4.18) are derived. These results further refine the calculation of the Page curve for Kerr–Newman black holes in *asymptotically flat* spacetime.

However, as mentioned in the introduction, the island formula is rigorously derived from the replica wormholes in the *asymptotically AdS* spacetime via the Euclidean path integral [16–18]. In addition, the first successful reproduc-

tion of the Page curve was achieved in the asymptotic AdS_2 Jackiw-Teitelboim black hole coupled to a non-gravitational thermal bath [8–10,21]. Although in this paper we obtain unitray results by applying the island formula in the context of asymptotically flat spacetime, caution remains warranted when addressing the black hole information paradox in asymptotically flat spacetime.

The first issue pertains to the dependence on spacetime. A significant portion of recent progress has largely focused on the Euclidean path integral [16–18]. These studies employ the replica wormholes to compute the entanglement entropy as a function of Euclidean coordinates. Subsequently, they analytically continuing the results to real times. These discussions continue to rely significantly on the AdS/CFT duality or related theoretical frameworks. Even in the analysis of *asymptotically flat* spacetime presented in [23–28]. This dependence persists, as demonstrated by the authors through an analogy with the AdS/CFT correspondence. However, this reliance on AdS/CFT correspondence gives rise to a important issue: the physical properties of wormholes lead to the so-called "factorization problem", which challenges the consistent interpretation of AdS/CFT [128]. The relevant paper [129] centers on operationally defined physical quantities-specifically, the measurement outcomes obtained by asymptotic observers-and carries out a comprehensive analysis strictly in the framework of the Lorentzian signature. This approach does not incorporate extra holographic (AdS/CFT) assumptions or presuppose inputs related to ultraviolet aspects of quantum gravity. Although the final result remains consistent with the unitary property of black hole evolution. However, the validity of this theory remains to be further evaluated. Consequently, one still needs to be cautious when dealing with the Page curve in asymptotically flat spacetime.

Another serious challenge is the *massive gravity* resulting from the entanglement island. Note that in the asymptotically flat spacetime with *massless gravitons*, long-range gravity and non-locality of the operator algebra associated with the entanglement wedge of island leads to inconsistency even in asymptotically flat spacetime coupled to a non-gravitational bath [130]. Therefore, caution must be exercised when using the island formula in such cases. Recently, issues pertaining to this point have generated considerable discussions. Reference [131] elucidates the emergence of entangled islands in the context of massless gravitons in systems without the auxiliary bath, and presents several specific examples to illustrate this explanation. It is suggested that, in all cases, the Page curve is physically observable and can be ascertained through sufficiently precise experiments conducted on multiple copies of the black hole. When the island rule is applied, these findings (combined with entanglement wedge reconstruction) demonstrate that semi-classical operators in the island region can be effectively approximated by nonperturbative operators acting on the Hawking radiation [131]. However, there are also some counterarguments. As mentioned in [132], the existing structure of entanglement islands (at least in the study of black hole physics) are all be established in the *massive gravity*. Indeed, reference [132] indicates that the mass of gravitons is not accidental but constitutes a necessary condition for the consistency of the holographic interpretation of entangled islands. An important insight from these studies is that the mass of the graviton reflects a profound connection between quantum entanglement and emergent spacetime geometry, as encapsulated by the "EPR=ER" conjecture [133]. Nevertheless, several intriguing questions and objections have been raised concerning the physical relevance of this relationship. The reference [132] asserts that either the definition of entangled islands should be revised, or the notion of a physically meaningful mass of graviton should be rejected.

Therefore, the scope of applicability of the island formula remains an open question that needs further investigation. Discussion on this aspect is beyond the scope of this paper. To further substantiate the calculations presented in our paper, we provide a detailed analysis of entangled islands in the Kerr Newman anti-de Sitter (KN-AdS) spacetime. These results offer valuable insights that may inform and guide future investigations in this field.

The Penrose diagram of KN-AdS coupled the auxiliary non-gravitational bath is drawn in Fig. 7 below. Different from the case of the asymptotical flat spacetime as shown in Fig. 2. The boundary located at infinity reflects the Hawking radiation emitted from the black hole. To cause black holes in the bulk to evaporate, we couple a non-gravitational thermal bath at the asymptotic boundary and impose transparent boundary conditions there. This setup ensures that the whole spacetime still approximates the situation in asymptotically flat spacetime. Consequently, the Hawking radiation can traverse the boundary and enter the bath region, and can be collected by the asymptotic observer.

Now we can calculate the entanglement entropy by the island formula in KN-AdS spacetime. The bulk metric is written as

$$\begin{aligned} ds^2(\text{bulk}) &= -\frac{\Delta_r}{\rho^2}\left(dt - \frac{a\sin^2\theta}{\Sigma}d\phi\right)^2 + \frac{\rho^2}{\Delta_r}dr^2 + \frac{\rho^2}{\Delta_\theta}d\theta^2 \\ &\quad + \frac{\Delta_\theta}{\rho^2}\sin^2\theta\left(adt - \frac{r^2+a^2}{\Sigma}d\phi\right)^2, \end{aligned} \tag{5.1}$$

where

$$\Delta_r = (r^2+a^2)\left(1+\frac{r^2}{\ell^2}\right) - 2mr + q^2, \tag{5.2a}$$

$$\Delta_\theta = 1 - \frac{a^2}{\ell^2}\cos 2\theta, \tag{5.2b}$$

$$\rho^2 = r^2 + a^2\cos^2\theta, \tag{5.2c}$$

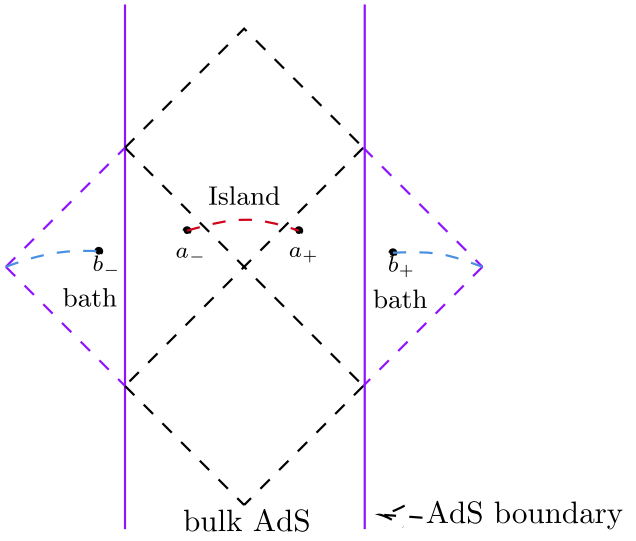

Fig. 7 The Penrose diagram of KN-AdS spacetime in thermal equilibrium with the bath. The black region tepresents the KN-AdS spacetime where the gravitational coupling is strong. While the purple region represents the auxiliary flat spacetime. The whole spacetime approximates an asymptotically flat black hole spacetime. The boundaries of radiation are labeled as $b_\pm$, and the boundaries of islands are $a_\pm$

$$\Sigma = 1 - \frac{a^2}{\ell^2}. \tag{5.2d}$$

Here ℓ is related to the renormalized cosmological constant $\Lambda \equiv -1/\ell^2$. When $1/\ell^2 = 0$, the bulk metric (5.1) reduces the Kerr Newman metric (2.1). The parameter m, q is related to the physical mass M, angular momentum J and charges Q of black hole

$$M = \frac{m}{\Sigma^2}, \qquad J = \frac{ma}{\Sigma^2}, \qquad Q = \frac{q}{\Sigma}. \tag{5.3}$$

The gauge potential is

$$A = -\frac{qr}{\rho^2}\left(dt - \frac{a\sin^2\theta}{\Sigma}d\phi\right), \tag{5.4}$$

and the field strength is

$$F = -\frac{1}{\rho^4}[q(r^2 - a^2\cos^2\theta) + 2qra\cos\theta] \left(dt - \frac{s\sin^2\theta}{\Sigma}d\phi\right) \wedge dr. \tag{5.5}$$

The bath region is nothing but the Minkowski spacetime

$$ds^2(\text{bath}) = -dt^2 + dr^2. \tag{5.6}$$

In addition, the Hawking temperature, Bekenstein–Hawking entropy and angular velocity of the event horizon are respectively

$$\hat{T}_H = \frac{r_+\left(1 + \frac{a^2}{\ell^2} + \frac{3r_+^2}{\ell^2} - \frac{a^2+q^2}{r_+^2}\right)}{4\pi(r_+^2 + a^2)}, \tag{5.7a}$$

$$\hat{S}_{\text{BH}} = \frac{\pi(r_+^2 + a^2)}{\Sigma G_N}, \tag{5.7b}$$

$$\hat{\Omega}_H = \frac{a\Sigma}{r_+^2 + a^2}. \tag{5.7c}$$

For simplicity, we follow the logic of the Sect. 4. We still consider the near extremal black hole and consider the near horizon geometry.[2] Similar to the Kerr Newman black hole (4.3), we take the following coordinate transformation [134]

$$r = \frac{r_+ + r_\star}{2} + \epsilon r_0\hat{r}, \qquad r_+ - r_\star = \lambda\epsilon r_0, \qquad t = \hat{t}\frac{r_0}{\epsilon}, \qquad \phi = \hat{\phi} + \Omega_H\hat{t}\frac{r_0}{\epsilon}, \tag{5.8}$$

where

$$k = 1 + \frac{a^2}{\ell^2} + \frac{6r_+^2}{\ell^2}, \tag{5.9a}$$

$$r_\star = r_+ - \frac{1}{kr_+}\left(r_+^2 - a^2 + \frac{3r_+^4}{\ell^2} + \frac{a^2r_+^2}{\ell^2}\right). \tag{5.9b}$$

Then the bulk metric can be reduce to a simple form, i.e., we can obtain the near horizon geometry of near extremal KN-AdS spacetime [135]

$$ds^2 = \Gamma(\theta)\Bigg(-\left(\hat{r} - \frac{\lambda}{2}\right)\left(\hat{r} + \frac{\lambda}{2}\right)d\hat{t}^2 + \frac{d\hat{r}^2}{\left(\hat{r} - \frac{\lambda}{2}\right)\left(\hat{r} + \frac{\lambda}{2}\right)} + \alpha(\theta)d\theta^2\Bigg) + \Lambda(\theta)(d\hat{\phi} + \hat{p}d\hat{t})^2, \tag{5.10}$$

where λ is defined by (5.8). The parameters are defined by

$$\Gamma(\theta) = \frac{\rho_+^2 r_0^2}{r_+^2 + a^2}, \quad \alpha(\theta) = \frac{r_+^2 + a^2}{\Delta_\theta r_0^2}, \quad \Lambda(\theta) = \frac{\Delta_\theta\sin^2\theta(r_+^2 + a^2)^2}{\rho_+^2 r_0^2}, \tag{5.11a}$$

$$\hat{p} = \frac{ar_0^2\Sigma(r_+ + r_\star)}{(r_+^2 + a^2)^2}, \quad \rho_+^2 = r_+^2 + a^2\cos^2\theta, \quad r_0^2 = \frac{r_+^2 + a^2}{k}. \tag{5.11b}$$

[2] The main purpose of our calculations in this section is to complement the analysis of the AdS spacetime scenario. For convenience, we consider the near extremal near horizon geometry, which markedly simplifies the mathematical treatment while preserving the underlying physical significance.

At last, at the $\theta = 0$ hypersurface, we obtain the co-dimension two geometry:

$$ds^2 = r_0^2\Big(-\Big(\hat{r}-\frac{\lambda}{2}\Big)\Big(\hat{r}+\frac{\lambda}{2}\Big)d\hat{t}^2 + \frac{d\hat{r}^2}{\Big(\hat{r}-\frac{\lambda}{2}\Big)\Big(\hat{r}+\frac{\lambda}{2}\Big)}\Big). \tag{5.12}$$

Similar (4.6), this metric is also contains the warp AdS_3.

In the end, we calculate the entanglement entropy under this metric (5.12) as the material. Similarly, by the Kruskal coordinate transformation (2.20), the metric can be extended to a conformal flat form

$$ds^2 = -\hat{\Omega}^{-2}(\hat{r})dUdV, \tag{5.13}$$

with the conformal factor and the tortoise coordinate

$$\hat{\Omega}^2(\hat{r}) = \frac{\lambda^2 e^{\lambda\hat{r}_\star}}{4r_0^2(\hat{r}^2-\frac{\lambda^2}{4})}, \qquad \hat{r}_\star(\hat{r}) = \frac{1}{\lambda}\log\frac{\hat{r}-\frac{\lambda}{2}}{\hat{r}+\frac{\lambda}{2}}. \tag{5.14}$$

In the configuration without island, the entropy is dominated by the radiation (see Fig. 7). Similar the calculation in (4.11), we have

$$S_R^{\text{no-island}}(\text{AdS}) = \frac{c}{3}\log[L(b_+,b_-)] \simeq \frac{2c}{3}\hat{T}_H t_b. \tag{5.15}$$

Then, for the island configuration, the generalized entropy is

$$\begin{aligned} S_{\text{gen}}(\text{AdS}) &= 2\frac{\text{Area}(\partial I)}{4G_N} - 2\gamma c\frac{\text{Area}(\hat{r}_b)}{L^2(a_+,b_+)} \\ &= \frac{2\pi(\hat{r}_a^2+a^2)}{\Sigma G_N} - \frac{4\gamma c\pi\hat{r}_b^2}{r_0^2\sqrt{(\hat{r}_a^2-\frac{\lambda^2}{2})(\hat{r}_b^2-\frac{\lambda^2}{2})}\Big[\cosh[\kappa(\hat{r}_\star(\hat{r}_a)-\hat{r}_\star(\hat{r}_b))]-\cosh[\kappa(\hat{t}_a-\hat{t}_b)]\Big]}. \end{aligned} \tag{5.16}$$

Extremizing the equation with respect to time $\hat{t}_a$, we obtain

$$\frac{\partial}{\partial\hat{t}_a}S_{\text{gen}}(\text{AdS}) \propto \sinh\left(\frac{\hat{t}_a-\hat{t}_b}{r_h}\right) = 0, \tag{5.17}$$

which implies that $\hat{t}_a = \hat{t}_b$. Then we invoke this relation to the generalized entropy and extremize it by the near-horizon approximation,

$$\begin{aligned} \frac{\partial}{\partial\hat{r}_a}S_{\text{gen}}(\text{AdS}) &= \frac{4\pi\hat{r}_a}{\Sigma G_N} \\ &- \frac{2c\pi\hat{r}_a(\frac{\lambda}{2}-\hat{r}_b)(\frac{\lambda}{2}+\hat{r}_b)\hat{r}_b^2\gamma\,\text{csch}\left[\frac{\kappa}{2}\left(\frac{1}{\hat{r}_b}-\frac{1}{\hat{r}_a}\right)\right]^2}{r_0^2\hat{r}_a^3\hat{r}_b^3} = 0. \end{aligned} \tag{5.18}$$

We solve this equation and eventually obtain the location of island is

$$\hat{r}_a \simeq r_0 + \frac{G_N\gamma c\pi(\frac{\lambda}{2}-\hat{r}_b)}{2r_0^2(a^2+r_0^2)\pi}. \tag{5.19}$$

At last, the entanglement entropy with island in KN-AdS metric is

$$S_R^{\text{island}}(\text{AdS}) \simeq \frac{2\pi(\hat{r}_0^2+a^2)}{\Sigma G_N} + \mathcal{O}(G_N) \simeq 2\hat{S}_{\text{BH}}. \tag{5.20}$$

Therefore, for the KN-AdS metric (5.12), we still obtain the unitary result by considering the island (5.19).

6 Discussion and conclusion

In summary, we study the information paradox in the four-dimensional Kerr–Newman spacetime. Due to the fact that the Kerr–Newman black hole represents a non-spherically symmetric higher dimensional spacetime (2.1), we initially prove that the quantum field in this spacetime can be equivalently described by an effective two-dimensional theory (2.18) in the near-horizon region. Then the entanglement entropy can be well approximated by CFT_2 in this framework. According to the island paradigm, the fine-grained entropy of Hawking radiation corresponds to the minimum value among the extremal values of the generalized entropy. We first concentrate on the non-extremal black hole. At early times, black holes have just formed, no island structures are present (3.8). This leads to the entanglement entropy is contributed by the radiation region and increases linearly with time (3.3), which sharpen the information paradox. By introducing the entanglement island at late times, the entanglement entropy is eventually dominated by the area term and gradually reaches the saturated Bekenstein–Hawking entropy (3.16). Based on these findings, we successfully reproduce the Page curve in Fig. 3 and accurately determine both the Page time (3.17) and the scrambling time (3.20). We also investigate the impact of the charge Q and the angular momentum a on these physical quantities (Figs. 4 and 5). When the charge Q is fixed, both the Page time and the scrambling time increases as the angular momentum increases. Conversely, when the angular momentum a is fixed, both the Page time and the scrambling time decreases as the charge inverses. In particular, for the critical cases when $a = 0$ (RN black holes) and $Q = 0$ (Kerr black holes), our results are consistent with [60,61]. However, when the black hole reaches the near extremal case, both the Page time and the scrambling time are approaching divergent. Therefore, we further investigate the situation of near extremal

Kerr–Newman black holes. According to the Kerr/CFT correspondence [120], the geometry of the near extremal Kerr–Newman black hole in the near-horizon limit is equivalent to a warped AdS_3 (4.4). Then we can still correctly evaluate the entropy to adapt the CFT_2 in the background for fixed θ (4.6). Furthermore, in the framework of this near extremal near-horizon geometry, the region incorporates an AdS_2 component characterized by enhanced $SL(2, R)$ symmetry. This structure accommodates a set of zero modes associated with large diffeomorphisms and gauge transformations, giving rise to strong coupling effects that modify the partition function by one-loop effects [124,125]. So the thermodynamic quantities with logarithmic correction are obtained (4.7) (4.8). The we reevaluate the entanglement entropy under these corrections. Similar to the non-extremal case, in the configuration without island, the entanglement entropy still grow linearly with time even in the extremal case (4.11). Subsequent, by taking account of islands, we conclude that the entanglement entropy is still bounded by the Bekenstein–Hawking entropy by the island formula even in the extremal case with vanishing temperature (4.16). Significantly, we also find that both the Page time (4.17) and the scrambling time (4.18) for near extremal black holes are delayed. This suggests that the near extremal limit not only corresponds to the geometric formation of AdS_2 in the near-horizon region of the Kerr–Newman black hole, but also signifies the domain dominated by Schwarzian dynamics, reflecting the quantum fluctuation of the gravitational system. These conclusions aligns with the principle that the entanglement entropy of a finite system remains finite, which also implies the validity of the island formula. In addition, we present a comprehensive discussion of the scope of applicability of the island formula. Although the island prescription has been applied to asymptotically flat spacetimes, its original derivation is firmly grounded in asymptotically AdS spacetimes with specific boundary conditions [16–18]. To ensure conceptual and technical rigor, we independently rederive the island construction in the KN–AdS spacetime given in (5.1). Within this framework, the evolution of the entanglement entropy is found to remain unitary, as shown in (5.20). These findings may serve as a reference for future studies in this field. Therefore, Our study broadens the application scope of the island formula and offers a systematic calculation method of the Page curve in the most general stationary spacetime. This work holds great potential value for future studies.

For the future research, a nice motivation is to study the evolution of entanglement entropy of evaporating Kerr–Newman black holes. It is anticipated that the emergence of islands will lead to the entropy drops to zero at the end of evaporation. Another interesting aspect to explore is the comtribution of superradiance to the Page curve. The superradiance of BTZ black holes has been studied previously in [79]. We intend to consider the superradiance into our analysis to further study the effects of charges and angular momentum on the Page curve. The final and most significant point concerns the issue of gravitons acquiring mass as implied by the island formula [130–132]. Currently, there is no consensus on this question, and it remains a key focus for future research in this field.

Acknowledgements We would like to thank Jun Nian, Yu Tian and Yi Ling for helpful discussions. The study was partially supported by NSFC, China (Grant No.12275166, No.12311540141 and No.12547142).

Data Availability Statement This manuscript has no associated data. [Authors' comment: Data sharing not applicable to this article as no datasets were generated or analysed during the current study.]

Code Availability Statement This manuscript has no associated code/software. [Authors' comment: Code/Software sharing not applicable to this article as no code/software was gen- erated or analysed during the current study.]

Funded by SCOAP[3].

References

1. S.W. Hawking, Particle creation by black holes. Commun. Math. Phys. **43**, 199 (1975). [Erratum: Commun. Math. Phys. 46, 206 (1976)]
2. W.G. Unruh, Notes on black hole evaporation. Phys. Rev. D **14**, 870 (1976)
3. S.W. Hawking, Breakdown of predictability in gravitational collapse. Phys. Rev. D **14**, 2460–2473 (1976)
4. J.D. Bekenstein, A universal upper bound on the entropy to energy ratio for bounded systems. Phys. Rev. D **23**, 287 (1981)
5. D.N. Page, Information in black hole radiation. Phys. Rev. Lett. **71**, 3743–3746 (1993). arXiv:hep-th/9306083
6. D.N. Page, Time dependence of Hawking radiation entropy. JCAP **1309**, 028 (2013). arXiv:1301.4995
7. J. Maldacena, The large N limit of superconformal field theories and supergravity. Int. J. Theor. Phys. **38**, 1113–1133 (1999). arXiv:hep-th/9711200
8. A. Almheiri, N. Engelhardt, D. Marolf, H. Maxfield, The entropy of bulk quantum fields and the entanglement wedge of an evaporating black hole. JHEP **12**, 063 (2019). arXiv:1905.08762
9. A. Almheiri, R. Mahajan, J. Maldacena, Y. Zhao, The Page curve of Hawking radiation from semiclassical geometry. JHEP **03**, 149 (2020). arXiv:1908.10996

10. G. Penington, Entanglement wedge reconstruction and the information paradox. JHEP **09**, 002 (2020). arXiv:1905.08255
11. A. Almheiri, T. Hartman, J. Maldacena, E. Shaghoulian, A. Tajdini, The entropy of Hawking radiation. Rev. Mod. Phys. **93**, 35002 (2021). arXiv:2006.06872
12. N. Engelhardt, A. Wall, Quantum extremal surfaces: holographic entanglement entropy beyond the classical regime. JHEP **01**, 073 (2015). arXiv:1408.3203
13. S. Ryu, T. Takayanagi, Holographic derivation of entanglement entropy from AdS/CFT. Phys. Rev. Lett. **96**, 181602 (2006). arXiv:hep-th/0603001
14. S. Ryu, T. Takayanagi, Aspects of holographic entanglement entropy. JHEP **08**, 045 (2006). arXiv:hep-th/0605073
15. A. Lewkowycz, J. Maldacena, Generalized gravitational entropy. JHEP **08**, 090 (2013). arXiv:1304.4926
16. G. Penington, S. Shenker, D. Stanford, Z. Yang, Replica wormholes and the black hole interior. JHEP **03**, 205 (2022). arXiv:1911.11977
17. A. Almheiri, T. Hartman, J. Maldacena, E. Shaghoulian, A. Tajdini, Replica wormholes and the entropy of Hawking radiation. JHEP **05**, 013 (2020). arXiv:1911.12333
18. K. Goto, T. Hartmana, A. Tajdini, Replica wormholes for an evaporating 2D black hole. JHEP **04**, 289 (2021). arXiv:2011.09043
19. C. Teitelboim, Gravitation and Hamiltonian structure in two space-time dimensions. Phys. Lett. B **126**, 41 (1983)
20. R. Jackiw, Lower dimensional gravity. Nucl. Phys. B **252**, 343 (1985)
21. A. Almheiri, R. Mahajan, J. Maldacena, Islands outside the horizon. arXiv:1910.11077
22. T. Hollowood, S. Kumar, Islands and Page curves for evaporating black holes in JT gravity. arXiv:2004.14944
23. T. Anegawa, N. Iizuka, Notes on islands in asymptotically flat 2d dilaton black holes. JHEP **07**, 036 (2020). arXiv:2004.01601
24. F. Gautason, L. Schneiderbauer, W. Sybesma, L. Thorlacius, Page curve for an evaporating black hole. JHEP **05**, 091 (2020). arXiv:2004.00598
25. T. Hartman, E. Shaghoulian, A. Strominger, Islands in asymptotically flat 2D gravity. JHEP **07**, 022 (2020). arXiv:2004.13857
26. X. Wang, R. Li, J. Wang, Islands and page curves for a family of exactly solvable evaporating black holes. Phys. Rev. D **103**, 126026 (2021). arXiv:2104.00224
27. R. Li, X. Wang, J. Wang, Island may not save the information paradox of Liouville black holes. Phys. Rev. D **104**, 106015 (2021). arXiv:2105.03271
28. M. Yu, X. Ge, Entanglement Islands in generalized two-dimensional dilaton black holes. Phys. Rev. D **107**, 066020 (2023). arXiv:2208.01943
29. C. Lu, M. Yu, X. Ge, Page curve and phase transition in deformed Jackiw–Teitelboim gravity. Eur. Phys. J. C **83**, 215 (2023). arXiv:2210.14750
30. J.F. Pedraze, A. Svesko, W. Sybesma, M.R. Visser, Microcanonical action and the entropy of Hawking radiation. Phys. Rev. D **105**, 126010 (2022). arXiv:2111.06912
31. J.F. Pedraze, A. Svesko, W. Sybesma, M.R. Visser, Semi-classical thermodynamics of quantum extremal surfaces in Jackiw–Teitelboim gravity. JHEP **12**, 134 (2021). arXiv:2107.10358
32. T. Hartman, Y. Jiang, E. Shaghoulian, Islands in cosmology. JHEP **11**, 111 (2020). arXiv:2008.01022
33. V. Balasubramanian, A. Kar, T. Ugajin, Islands in de Sitter space. JHEP **02**, 072 (2021). arXiv:2008.05275
34. W. Sybesma, Pure de Sitter space and the island moving back in time. Class. Quantum Gravity **38**, 145012 (2021). arXiv:2008.07994
35. H. Geng, Y. Nomura, H. Sun, Information paradox and its resolution in de sitter holography. Phys. Rev. D **103**, 126004 (2021). arXiv:2103.07477
36. L. Aalsma, W. Sybesma, The price of curiosity: information recovery in de Sitter space. JHEP **05**, 291 (2021). arXiv:2104.00006
37. Y. Chen, V. Gorbenko, J. Maldacena, Bra-ket wormholes in gravitationally prepared states. JHEP **02**, 009 (2021). arXiv:2007.16091
38. M.V. Raamsdonk, Comments on wormholes, ensembles, and cosmology. JHEP **12**, 156 (2021). arXiv:2008.02259
39. S. Azarnia, R. Fareghbal, A. Naseh, H. Zolfi, Islands in flat-space cosmology. Phys. Rev. D **104**, 126017 (2021). arXiv:2109.04795
40. V. Balasubramanian, A. Kar, T. Ugajin, Entanglement between two disjoint universes. JHEP **02**, 136 (2021). arXiv:2008.05274
41. A. Miyata, T. Ugajin, Evaporation of black holes in flat space entangled with an auxiliary universe. arXiv:2104.00183
42. V. Balasubramanian, A. Kar, T. Ugajin, Entanglement between two gravitating universes. Class. Quantum Gravity **39**, 174001 (2022). arXiv:2104.13383
43. R. Espindola, B. Najian, D. Nikolakopoulou, Islands in FRW cosmologies. arXiv:2203.04433
44. Q. Hu, D. Li, R. Miao, Y. Zeng, AdS/BCFT and Island for curvature-squared gravity. JHEP **09**, 037 (2022). arXiv:2202.03304
45. P. Hu, D. Li, R. Miao, Island on codimension-two branes in AdS/dCFT. JHEP **11**, 008 (2022). arXiv: 2208.11982
46. R. Miao, Entanglement island versus massless gravity. Eur. Phys. J. C **84**, 123 (2024). arXiv:2212.07645
47. R. Miao, Entanglement island and Page curve in wedge holography. JHEP **03**, 214 (2023). arXiv:2301.06285
48. D. Li, R. Miao, Massless entanglement islands in cone holography. JHEP **06**, 056 (2023)
49. Y. Guo, R. Miao, Page curves on codim-m and charged branes. Eur. Phys. J. C **83**, 847 (2023)
50. Y. Shao, M. Yuan, Y. Zhou, Entanglement negativity and defect extremal surface. SciPost Phys. Core **7**, 027 (2024). arXiv:2206.05951
51. T. Li, J. Chu, Y. Zhou, Reflected entropy for an evaporating black hole. JHEP **11**, 155 (2020). arXiv:2006.10846
52. T. Li, M.K. Yuan, Y. Zhou, Defect extremal surface for reflected entropy. JHEP **01**, 018 (2022). arXiv:2108.08544
53. T.J. Hollowood, S.P. Kumar, A. Legramandi, Hawking radiation correlations of evaporating black holes in JT gravity. J. Phys. A: Math. Theor. **53**, 475401 (2020). arXiv:2007.04877
54. M. Alishahiha, A. Faraji Astaneh, A. Naseh, Island in the presence of higher derivative terms. JHEP **02**, 035 (2021). arXiv:2005.08715
55. J. Chu, F. Deng, Y. Zhou, Page curve from defect extremal surface and island in higher dimensions. JHEP **10**, 149 (2021). arXiv:2105.09106
56. Z. Wang, Z. Xu, S. Zhou, Y. Zhou, Partial reduction and cosmology at defect brane. JHEP **05**, 049 (2022). arXiv:2112.13782
57. F. Deng, Y. An, Y. Zhou, JT gravity from partial reduction and defect extremal surface. JHEP **02**, 219 (2023). arXiv:2206.09609
58. F. Deng, Z. Wang, Y. Zhou, End of the world brane meets $T\bar{T}$. JHEP **07**, 036 (2024). arXiv:2310.15031
59. K. Hashimoto, N. Iizuka, Y. Matsuo, Islands in Schwarzschild black holes. JHEP **06**, 085 (2020). arXiv:2004.05863
60. X. Wang, R. Li, J. Wang, Islands and page curves of Reissner–Nordström black holes. JHEP **04**, 103 (2021). arXiv:2101.06867
61. L. Wang, R. Li, Entanglement islands and the page curve of Hawking radiation for rotating Kerr black holes. Phys. Rev. D **110**, 06601 (2024)
62. S. Azarnia, R. Fareghbal, Islands in Kerr–de Sitter spacetime and their flat limit. Phys. Rev. D **106**, 026012 (2022)
63. B. Ahn, S.E. Bak, H.S. Jeong, K.Y. Kim, Y. Sun, Islands in charged linear dilaton black holes. Phys. Rev. D **105**, 046012 (2022)

64. W. Kim, M. Nam, Entanglement entropy of asymptotically flat non-extremal and extremal black holes with an island. Eur. Phys. J. C **81**, 869 (2021)
65. Y. Potaux, D. Sarkar, S.N. Solodukhin, Islands for black holes in a hybrid quantum state. arXiv:2411.09574
66. A. Shekar, M. Taylor, Replica analysis of entanglement properties. arXiv:2410.07312
67. A.I. Belokon, Finite entangling regions and information paradox in charged black holes. arXiv:2409.01409
68. H. Jeong, K. Kim, Y. Sun, Entanglement entropy analysis of dyonic black holes using doubly holographic theory. arXiv:2305.18122
69. Y. Ling, P. Liu, Y. Liu, C. Niu, Z. Xian, C. Zhang, Reflected entropy in double holography. JHEP **02**, 037 (2022). arXiv:2109.09243
70. Y. Liu, Z. Xian, C. Peng, Y. Ling, Black holes entangled by radiation. JHEP **09**, 179 (2022). arXiv:2205.14596
71. Y. Liu, Q. Chen, Y. Ling, C. Pend, Y. Tian, Z. Xian, Entanglement of defect subregions in double holography. arXiv:2312.08025
72. Y. Liu, S. Jian, Y. Ling, Z. Xian, Entanglement inside a black hole before the Page time. arXiv:2401.04706
73. C. Tong, D. Du, J. Sun, Island of Reissner–Nordström anti-de Sitter black holes in the large d limit. Phys. Rev. D **109**, 104053. arXiv:2306.06682
74. H. Geng, Graviton mass and entanglement islands in low spacetime dimensions. arXiv:2312.13336
75. H. Geng, A. Karch, C. Perez-Pardavila, S. Raju, L. Randall, M. Riojas, S. Shashi, Inconsistency of islands in theories with long-range gravity. JHEP **01**, 182 (2022). arXiv:2107.03390
76. H. Geng, Y. Nomura, H.Y. Sun, Information paradox and its resolution in de Sitter holography. Phys. Rev. D **103**(12), 126004 (2021)
77. H. Geng, The mechanism behind the information encoding for islands. arXiv:2502.08703
78. M. Yu, X. Ge, Islands and Page curves in charged dilaton black holes. Eur. Phys. J. C **82**(1), 14 (2022). arXiv:2107.03031
79. M. Yu, C. Lu, X. Ge, S. Sin, Island and Page curve, and superradiance of rotating BTZ black holes. Phys. Rev. D **105**(6), 066009 (2022). arXiv:2112.14361
80. M. Yu, X. Ge, C. Lu, Page curves for accelerating black holes. Eur. Phys. J. C **83**, 12 (2023). arXiv:2306.11407
81. S. Lin, M. Yu, X. Ge, L. Tian, Entanglement entropy, phase transition, and island rule for Reissner–Nordström-adS black holes. Phys. Rev. D **110**, 046008 (2024). arXiv: 2405.06873
82. M. Yu, X. Ge, Geometric constraints via Page curves: insights from island rule and quantum focusing conjecture. Chin. Phys. C **49**, 045107. arXiv:2405.03220
83. M. Yu, S. Lin, X. Ge, Replica wormholes, modular entropy, and capacity of entanglement in JT gravity. Sci. China Phys. Mech. Astron. **69**, 220412 (2026). https://doi.org/10.1007/s11433-025-2811-4
84. A. Chandra, Z. Li, Q. Wen, Entanglement islands and cutoff branes from path-integral optimization. JHEP **07**, 069 (2024). arXiv:2402.15836
85. A. Almheiri, R. Mahajan, J.E. Santos, Entanglement islands in higher dimensions. SciPost Phys. **9**(1), 001 (2020). arXiv:1911.09666
86. S. He, Y. Sun, L. Zhao, Y.X. Zhang, The universality of islands outside the horizon. JHEP **05**, 047 (2022). arXiv:2110.07598
87. C. Chou, H. Lao, Y. Yang, Page curve of effective Hawking radiation. Phys. Rev. D **106**(6), 066008 (2022). arXiv:2111.14551
88. B. Ahn, S. Bak, H. Jeong, K.Y. Kim, Y.W. Sun, Islands in charged linear dilaton black holes. Phys. Rev. D **105**, 046012 (2022). arXiv:2107.07444
89. J. Chang, S. He, Y. Liu, L. Zhao, Island formula in Planck brane. JHEP **11**, 006 (2023). arXiv:2308.03645
90. H. Zhong, Page transition as a phase transition in approximate quantum error correction. arXiv:2408.15104
91. Q. Wen, M. Xu H. Zhong, Partial entanglement entropy threads in island phase. arXiv:2408.13535
92. P.X. Hao, T. Kawamoto, S.M. Ruan, T. Takayanagi, Non-extremal island in de Sitter gravity. arXiv:2407.21617
93. Y. Matsuo, Universal structure of islands in evaporating black holes. arXiv:2407.20921
94. H. Singh, Kaluza–Klein discreteness of the entropy: symmetrical bath and CFT subsystem. arXiv:2407.13447
95. L. Wang, R. Li, Entanglement islands and the Page curve of Hawking radiation for rotating Kerr black holes. Phys. Rev. D **110**(6), 066012 (2024). arXiv:2406.13949
96. Y. Qu, Y. Lan, H. Yu, W. Gan, F. Shu, Entanglement island and Page curve for one-sided charged black hole. JHEP **08**, 023 (2024). arXiv:2405.16457
97. C. Guo, W. Gan, F. Shu, Page curves and entanglement islands for the step-function Vaidya model of evaporating black holes. JHEP **05**, 042 (2023)
98. W. Gan, D. Du, F. Shu, Island and page curve for one-sided asymptotically flat black hole. JHEP **07**, 020 (2022)
99. R. Bousso, G. Penington, Islands far outside the horizon. JHEP **11**, 164 (2024). arXiv:2312.03078
100. A. Ishibashi, Y. Matsuo, A. Tanaka, Quantum focusing conjecture in two-dimensional evaporating black holes. JHEP **09**, 126 (2024). arXiv:2403.19136
101. A.R. Chowdhury, A. Saha, S. Gangopadhyay, Role of mutual information in the Page curve. Phys. Rev. D **106**, 086019 (2022). arXiv:2207.13029
102. D. Basu, A. Chandra, H. Choursiya, Reflected entropy and islands in a braneworld cosmology. arXiv:2503.17819
103. A. Saha, A.R. Chowdhury, S. Gangopadhyay, Investigating the role of mutual information in the Page curve for a functional renormalization group improved Schwarzschild black hole. arXiv:2503.19475
104. Y. Liu, W. Xu, B. Zhang, Island rules for the noncommutative black hole. arXiv:2505.09157
105. X. Ge, Zeno's paradox and black hole information loss problem. Acta Phys. Sin. **74**(8), 081101 (2025)
106. A.R. Chowdhury, A. Saha, S. Gangopadhyay, Mutual information of subsystems and the Page curve for the Schwarzschild–de Sitter black hole. Phys. Rev. D **108**, 02003 (2023). aXiv:2303.14062
107. Y. Lin, J. Sun, Y. Sun, J. Jin, The PEE aspects of entanglement islands from bit threads. JHEP **07**, 009 (2022). arXiv:2203.0311
108. D. Du, W. Gan, F. Shu, J. Sun, Unitary constraints on semiclassical Schwarzschild black holes in the presence of Island. Phys. Rev. D **107**, 026005 (2023). arXiv:2206.10339
109. Y. Du, J. Sun, X. Zhang, Information paradox and island of covariant black holes in LQG. arXiv:2510.11921
110. A. Karch, H. Sun, C.F. Uhlemann, Double holography in string theory. JHEP **10**, 012 (2022). arXiv:2206.11292
111. C.F. Uhlemann, Islands and Page curves in 4d from type IIB. JHEP **08**, 104 (2021). arXiv:2105.00008
112. S.E. Aguilar-Gutierrez, R. Espindola, E.K. Morvan-Benhaim, A teleportation protocol in Schwarzschild-de Sitter space. JHEP **03**, 095 (2025). arXiv:2308.13516
113. K. Umetsu, Hawking radiation from Kerr–Newman black hole and tunneling mechanism. Int. J. Mod. Phys. A **25**, 4123–4140 (2010). arXiv:0907.1420
114. H. Casini, C.D. Fosco, M. Huerta, Entanglement and alpha entropies for a massive Dirac field in two dimensions. J. Stat. Mech. **0507**, P07007 (2005). arXiv:cond-mat/0505563
115. P. Hayden, J. Preskill, Black holes as mirrors: quantum information in random subsystems. JHEP **09**, 120 (2007). arXiv:0708.4025

116. Y. Sekino, L. Susskind, Fast scramblers. JHEP **10**, 065 (2008). arXiv:0808.2096
117. Q. Wang, M. Yu, X. Ge, Scrambling time for analogue black holes embedded in AdS space. Eur. Phys. J. C **82**, 468 (2022). arXiv:2203.07914
118. S. Carroll, M. Johnson, L. Randall, Extremal limits and black hole entropy. JHEP **11**, 109 (2009)
119. J. Preskill et al., Limitations on the statistical description of black holes. Mod. Phys. Lett. A **6**, 2353 (1991)
120. M. Guica, T. Hartman, W. Song, A. Strominger, The Kerr/CFT correspondence. Phys. Rev. D **880**, 124008 (2009). arXiv:0809.4266
121. J.D. Brown, M. Henneaux, Central charge in the canonical realization of asymptotic symmetries: an example from three-dimensional gravity. Commun. Math. Phys. **104**, 207 (1986)
122. J.M. Bardeen, G.T. Horowitz, The extreme Kerr throat geometry: a vacuum analog of $AdS_2 \times S^2$. Phys. Rev. D **60**, 104030 (1999). arXiv:hep-th/9905099
123. T. Hartman, K. Murata, T. Nishioka, A. Strominger, CFT duals for extreme black holes. JHEP **04**, 019 (2009). arXiv:0811.4393
124. D. Kapec, A. Sheta, A. Strominger, C. Toldo, Logarithmic corrections to Kerr thermodynamics. Phys. Rev. Lett. **133**, 021601 (2024). arXiv:2310.00848
125. A. Sen, Logarithmic corrections to rotating extremal black hole entropy in four and five dimensions. Gen. Relativ. Gravit. **44**, 1207 (2012). arXiv:1109.3706
126. L. Rakic, M. Rangamani, G.J. Turiaci, Thermodynamics of the near-extremal Kerr spacetime. JHEP **06**, 011 (2024)
127. G.J. Turiaci, New insights on near-extremal black holes. arXiv:2307.10423
128. S.B. Giddings, G.J. Turiaci, Wormhole calculus, replicas, and entropies. JHEP **09**, 194 (2020). arXiv:2004.02900
129. D. Marolf, H. Maxfield, Observations of Hawking radiation: the Page curve and baby universes. JHEP **04**, 272 (2021). arXiv:2010.06602
130. H. Geng, A. Karch, C. Perez-Pardavila, S. Raju, L. Randall, M. Riojas, S. Shashi, Inconsistency of islands in theories with long-range gravity. JHEP **01**, 182 (2022). arXiv:2107.03390
131. S. Antonini, C.H. Chen, H. Maxfield, G. Penington, An apologia for islands. arXiv:2506.04311
132. H. Geng, Making the case for massive islands. arXiv:2509.22775
133. J. Maldacena, L. Susskind, Cool horizons for entangled black holes. Fortschr. Phys. **61**, 781 (2013). arXiv:1306.0533
134. B. Chen, J. Long, On holographic description of the Kerr–Newman-AdS-dS black holes. JHEP **08**, 065 (2010). arXiv:1006.0157
135. J. Rasmussen, On the CFT duals for near-extremal black holes. Mod. Phys. Lett. A **26**, 1601 (2011). arXiv:1005.2255